Research Article: Open Access

DOI: 10.35840/2631-5092/4557

VIBGYOR ePress

International Journal of
Optics and Photonic Engineering

Optical Study of Hybrid Colloidal Solution Based on P3OT Polymer and Cdse Nanoparticles

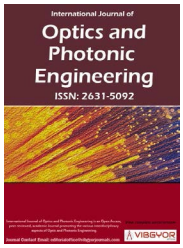

ISSN: 2631-5092

***A Benchaabane*[1,2*] *and A Lahmar*[3]**

[1]*Laboratoire de Science et Technologie pour la défense, Centre de Recherche Militaire, Académie Militaire, Tunisie*

[2]*École d'Aviation de Borj El Amri, route Mjez El Beb, 1142, Tunis, Tunisia*

[3]*Laboratoire de Physique de la Matière Condensée, Université de Picardie Jules Verne, Amiens, France*

Abstract

The effect of oleic acid-capped CdSe nanoparticles incorporation into poly(8-octylthiophene) (P3OT) colloidal solutions on optical properties was investigated. The photoluminescence study was carried out on both P3OT and P3OT:wt%CdSe solutions. The results showed that the inclusion of oleic acid-capped CdSe strongly influenced the fluorescence spectra. This trend was described within the Förster formalism, which involves a non-radiative energy transfer from the donor P3OT to the acceptor CdSe NPs. Furthermore, the P3OT solution with a high oleic acid-capped CdSe concentration level was found to exhibit a clear splitting, assigned to the existence of different emitting chromophore species. A modified Stern-Volmer model was used to interpret the fluorescence quenching in this system.

Keywords

Colloidal solution, Poly(8-octylthiophene)(P3OT), Oleic acid-capped cadmium selenide nanoparticles (CdSe)

Introduction

Conjugated conducting polymers (CPs), such as polypyrrole (PPy), polyaniline (Pani), and polythiophene (PTh) emerge as an alternative matrix for replacing silicon based materials. This interest resides in their flexible manufacturing and low-cost fabrication, which attracted much attention in both fundamental research and technological applications, especially in electronics and optoelectronics domains [1-4]. Besides, polythiophenes gained particular attentiveness because their end-group functionalization could lead to an attractive prospect of having a molecular handle for charge transfer, surface modification, self assembly, growth of block copolymers, and biomarking [5-7]. In addition, polythiophenes are environmentally stable, easily processed in solution, and can show good synthetic versatility including their regiospecific synthesis [8,9]. It should be noted however that the superiority of polytiophenes as promising organic materials depends upon the possibilities of being combined

***Corresponding author:** *A Benchaabane, Laboratoire de Science et Technologie pour la Défense, Centre de Recherche Militaire, Académie Militaire, Tunisie; Ecole d'Aviation de Borj El Amri, route Mjez El Beb, 1142, Tunis, Tunisia*

Accepted: January 29, 2024; **Published:** January 31, 2024

Citation: Benchaabane A, Lahmar A (2024) Optical Study of Hybrid Colloidal Solution Based on P3OT Polymer and Cdse Nanoparticles. Int J Opt Photonic Eng 9:057

with different inorganic nanoparticles (NPs) such as cadmium selenide (CdSe) [10], titanium dioxide (TiO_2) [11], ZnO [12], cadmium sulfide (CdS) [13] or other inorganic nanoparticles [14] to create organic/inorganic nanocomposites. This would, therefore, offer the possibility of achieving an unlimited variety of hybrid organic/inorganic materials with diverse functional properties and hence would open new horizons in advanced materials research [15,16]. In this context, hybrid materials composed of polymer and inorganic nanoparticles have shown excellent optoelectronic properties promising for potential applications such as photovoltaic cells (PV), light emitting diodes (LEDs), photodetectors, sensors, and transistors [11,17-20]. Numerous investigations reported that these applications benefit from improved carrier generation and enhanced charge transport as well as efficient exciton dissociation in PTh-containing organic/inorganic nanocomposites [21-28]. However, a particular interest is reserved to poly(octyltiophene) P3OT polymer and oleic acid (OA) capped CdSe NPs system [29-31] as bulk heterojunction (BHJ) photoactive layers in hybrid solar cells. It should be pointed out that the morphologies and distribution of the NPs in such a polymer matrix strongly influence the optical and electrical properties, and in particular the photovoltaic performances of the composites [32].

It is agreed upon that bulk heterojunction BHJ photovoltaic cells can be processed from liquid solution where the chemical synthetic process and molecular design play an important role for their efficiency [33,34]. However, most of the investigations were carried out mainly on optical properties of BHJ thin films rather than on starting solutions, which play a key role for predicting the performance of final BHJ solar cell thin films.

In the present work, we focus more particularly on the study of the influence of oleic acid- capped CdSe NPs incorporation into P3OT matrix in solution state. We use photoluminescence analysis as a preferential tool to study the charge transfer occurring at the donor-acceptor interface. The effect of NPs concentration on photoluminescence properties is also discussed.

Experimental

For the colloidal solution preparation, the first step consists of the preparation of CdSe nanoparticules (NPs) from a mixture of equal volume ratio of cadmium acetate and oleic acid in diphenyl ether. The NPs are capped with oleic acid by precipitation with copious amounts of methanol and are collected by centrifugation and decantation as previously reported for ZnSe [35].

The precipitated nanoparticles were recovered by adding a small amount of chloroform and reprecipitated with methanol. This purification process was repeated three times with a dilution in chloroform (20 g/l) and the obtained solution

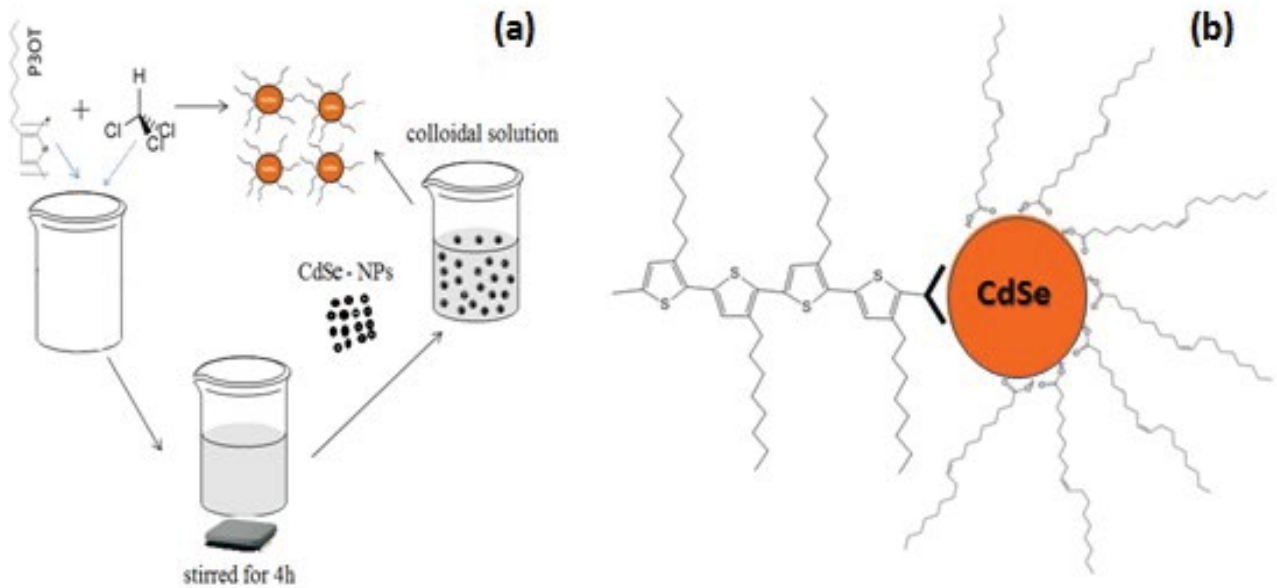

Figure 1: (a) A schematic description of experimental set up for the preparation of P3OT:wt%CdSe colloidal solution. (b) Schematic diagram of electronic interaction of CdSe NPs with P3OT polymer.

was stirred for 4h at room temperature to increase the solubility of P3OT. The composite solution was then prepared by adding CdSe nanoparticles to P3OT solution. For our study, five different nanocomposites were prepared corresponding to the concentrations 0 wt% (pure polymer), 20, 40, 60 and 80 wt% of CdSe, respectively (Figure 1a). Figure 2b describes the obtained P3OT:CdSe hybrid materials.

X-rays diffraction analysis was carried out on the CdSe powder using a Bruker D4 Diffractometer (lambda $K\alpha_1$ = 1.54056 Å, lambda $K\alpha_2$ = 1.54439 Å) operating at 40 kV and 40 mA. The morphologies and size of CdSe- NPs were examined by a transmission electron microscope (FEI Tecnai G2 20). The photoluminescence (PL) spectra for all investigated solutions were obtained using a LS 55 Fluorescence Spectrometer (PerkinElmer) with a 400 nm excitation wavelength.

Results and Discussion

Figure 2a represents the XRD diffractogram of CdSe NPs sample powder, which shows three main broad diffraction peaks, of cubic zincblend CdSe located at 25.7°, 42.3° and 49.8° corresponding to the favorite orientations (111), (220) and (311), respectively. All Bragg's reflections well matched the previously reported literature values [36] and prove thecrystallinity of CdSe NPs. The average crystallite size of CdSe was calculated from the highest peaks intensity by using Debye Scherrer's equation [37]:

$$D = \frac{0.9\lambda}{\beta\cos\theta}$$

Where D is the nanoparticle size, λ is the X-ray wavelength of 1.5406 Å, β is the corrected full width at half maximum (FWHM) of the coherent domain along a direction normal and θ is Bragg diffraction angle of the most intense peaks.

By applying the Scherrer equation for the three peaks, CdSe NPs size values of 6.5, 10.3 and 6.3 nm, respectively were obtained. An average value of (8 ± 2) nm was deduced, which agrees with those reported in previous works [38,39]. The size of NPs is also confirmed with transmission electron microscopy (TEM) image presented in Figure 2b, which clearly reveals a homogeneous dispersion of CdSe nanoparticles with an average diameter of (8 ± 5) nm.

Figure 3 represents comparative emission spectra of CdSeNPs and P3OT solutions. For cadmium selenide nanoparticles, the emission spectra under excitation of 400 nm show a maximum of emission at 2.18 eV. This maximum is significantly shifted compared to the results reported by Okamoto, et al. [40] for CdSe-based QDs (1.99 eV) in toluene solution. For instance, Ananthakumar, et al. [41] showed that the nature of the medium influences the absorption spectra of CdSe; the authors attributed this dependence to the medium dissociation constant and to the Gibbs

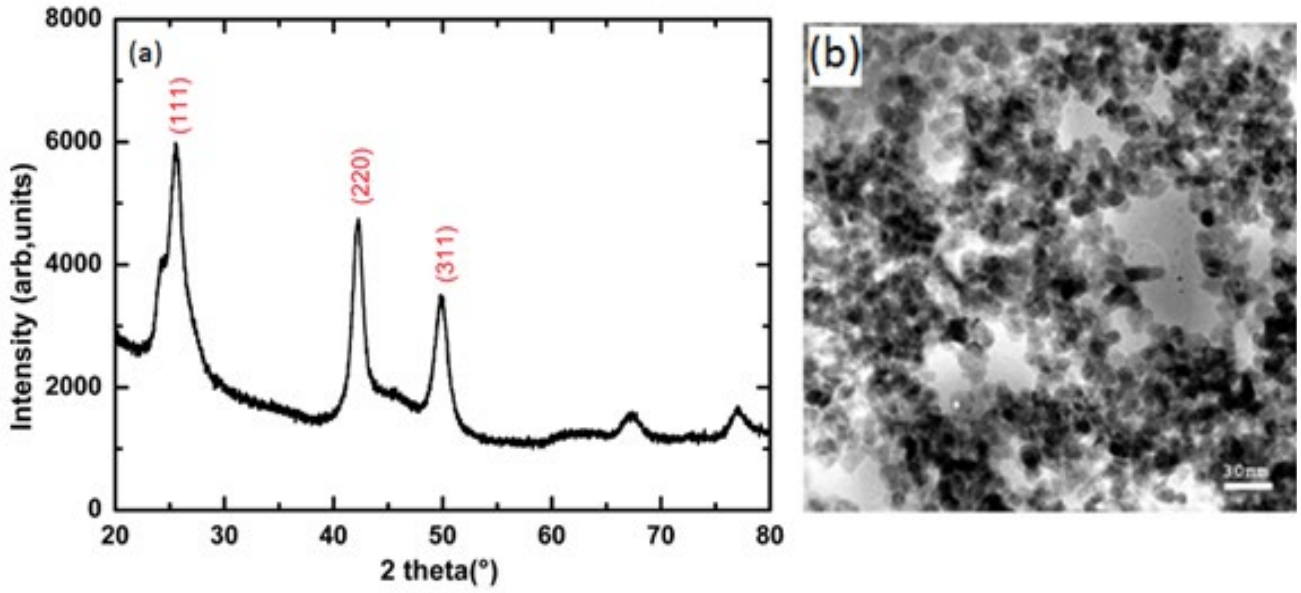

Figure 2: Powder X-ray diffraction pattern of CdSe NPs (a) TEM image of the prepared CdSe nanoparticles (b).

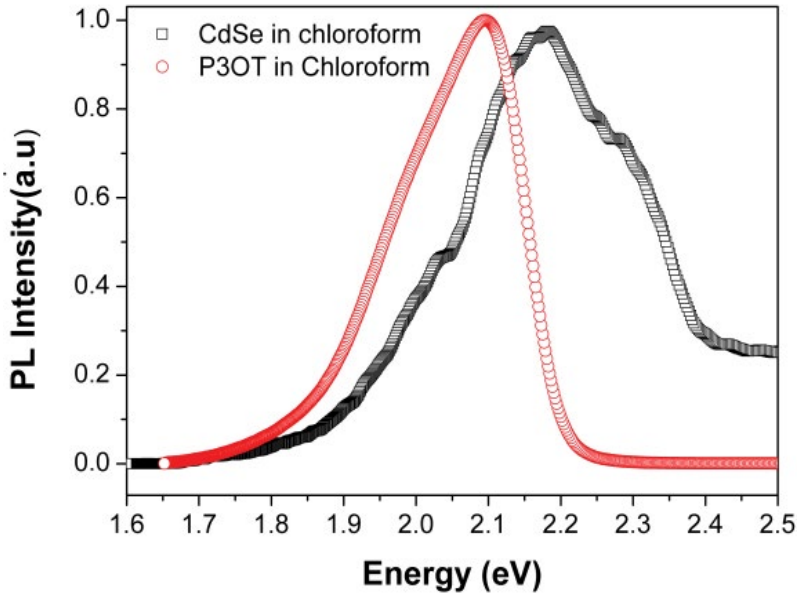

Figure 3: Photoluminescence spectra of CdSe-NPs and P3OT solutions.

free energy of the entire phase transfer process that could exist. For poly(8-octylthiophene), the emission band response is in the range of 1.8-2.2 eV, and no P3OT aggregates are detected for which the emission occurs in the range 1.3-1.8 eV [42]. The maximum of emission observed in our measurement is around 2.12 eV. In addition, the profile is not symmetric and a shoulder could be albeit detected around 2 eV. It should be noticed that the emission spectrum in solid state is generally expected to split because of the local single chain conformation and chain-chain interactions [43]. In our case, chloroform, which is a good solvent for the title polymer, might induce suppression of such interactions and only the solvent-solute interaction would be predominating.

To have a better understanding of the photoluminescence PL properties of pure P3OT polymer and P3OT:%CdSe hybrid material, the PL curves were analyzed using a multi-Gaussian functions, as shown in Figure 4. The profile of the photoluminescence band is typical of a multi-phonon process, i.e., a material in which the relaxation occurs by several paths, involving the participation of numerous states within the band gap of the material [44]. This behavior is probably related to the presence of additional electronic levels in the forbidden band gap of the material.

The P3OT spectrum displays four peaks of fluorescence centered at 2.12 eV (583 nm), 2.08 eV (595 nm), 2.01 eV (616 nm) and 1.92 eV (645 nm), respectively. We assume in the present work the existence of at least four bands characteristics for the invariable matrix ascribed to carbonyl-related chromophore groups that are inherent to P3OT. The analysis of the spectrum shows that the difference in the energy between consecutive peaks is in the range of 0.04-0.07 eV, which proves that the photoluminescence is governed by vibronic transitions [45]. Furthermore, the contribution centered at 583 nm (2.12 eV) can be attributed to the formation of the quinone structure, while that centered at 645 nm (1.92 eV) may be assigned to the pristine structure [46-48]. Moreover, the maxima situated at 2.08 eV and 2.01 eV are probably specific to vibronic transitions of the C=C stretching mode in the thiophene rings [49].

As it can be seen from Figure 5, the photoluminescence spectra of CdSe NPs show an intense emission peak at 567 nm with the presence of two other shoulders may be originate from the nom homogeneity of the NPs size. Kumari, et al. found a maximum of photoluminescence intensity at 550 nm for CdSe nanoparticles capped with oleic acid of size equal to 7 nm in toluene solution [50]. Sharma, et al. proved that oleic acid is a particular ligand that yields much more stable active metal nanoparticles than other saturated fatty acids. Moreover, they showed that OA passivates most of the vacancies and trap sites on the CdSe surface thus increasing the photostability of nanoparticles [51]. Gerou, et al. studied CdSe NPs emission spectrum

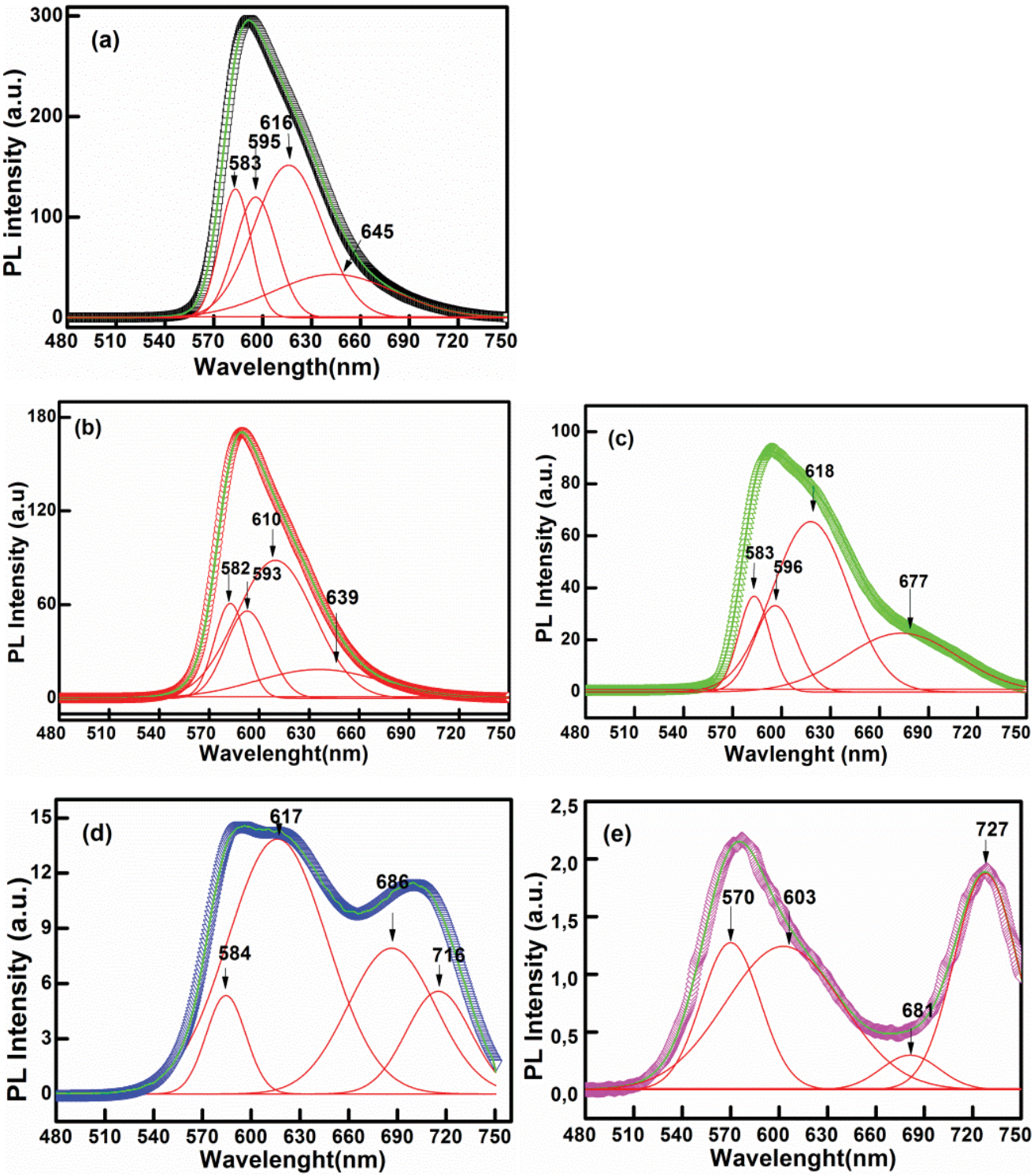

Figure 4: Deconvolution of PL curve, (a) P3OT, (b) P3OT:20% CdSe, (c) P3OT:40% CdSe, (d) P3OT:60% CdSe and (e) P3OT:80% CdSe samples.

with deconvolution method. The spectrum was decomposed into a main PL band, positioned at 543 nm and two weak bands shifted to the red, at 576 and 670 nm [52].

As shown in Figure 4a, the PL spectrum of pure P3OT polymer consists of four PL components. The first feature around 583 nm and the second at about 595 nm corresponding to a yellow component, the third one (≈ 616 nm) corresponds to orange component and the last peak (≈ 645 nm) corresponds to a red component."

The same order of colors is observed for

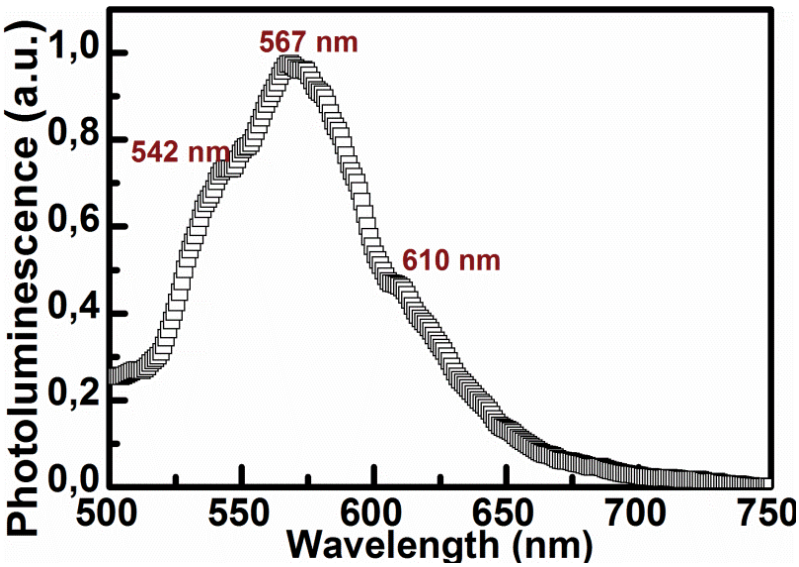

Figure 5: Photoluminescence spectrum of CdSe in chloroform as a function of wavelength.

Table 1: Photoluminescence peaks of pure P3OT and P3OT:wt% CdSe samples.

Sample	PL pick 1	PL pick 2	PL pick 3	PL pick 4
P3OT	583 nm (2.12 eV) yellow	595 nm (2.08 eV) yellow	616 nm (2.01 eV) orange	645 nm (1.92 eV) red
P3OT:20%CdSe	582 nm (2.13 eV) yellow	593 nm (2.09 eV) yellow	610 nm (2.03 eV) orange	639 nm (1.94 eV) red
P3OT:40%CdSe	583 nm (2.12 eV) yellow	596 nm (2.08 eV) yellow	618 nm (2.00 eV) orange	677 nm (1.83 eV) red
P3OT:60%CdSe	584 nm (2.12 eV) yellow	617 nm (2.00 eV) Orange	686 nm (1.80 eV) red	716 nm (1.73 eV) red
P3OT:80%CdSe	570 nm (2.17 eV) Yellow	603 nm (2.05 eV) Orange	681 nm (1.82 eV) red	727 nm (1.70 eV) red

P3OT:20%CdSe and P3OT:40%CdSe. Noting that each color represents different types of electronic transition linked to a specific structural molecule arrangement [53]. On the other hand, a red shift is observed for samples containing a large number of nanoparticles (P3OT:60%CdSe and P3OT:80%CdSe samples). The last peak (≈ 716-727 nm) observed for P3OT:60%CdSe and P3OT:80%CdSe samples, is attributed to red component color and it represents different types of electronic transition linked to a specific structural nanocomposite arrangement [53]. All the obtained components with the related assignment are gathered in Table 1.

Furthermore, we observe a slight red shift of the third and the fourth features (Figure 4d and Figure 4e). Such a behavior could be assigned to a large number of NPs incorporated in polymer matrix. Similar case is observed in P3EEET-ZnO nanocomposite reported by Huan-Ming Xiong where the red shift was attributed to NPs aggregation causing a significant decrease in polymer photoluminescence [54].

The PL intensity was at the maximum for pure P3OT and decreases with increasing CdSe NPs concentration (Figure 6a). The observed quenching phenomenon is mainly due to the concentration effect. However, one of the possible mechanisms that may occur, is the direct charge transfer between CdSe NPs and P3OT, leading to the formation of isolated electron-hole pairs. Such a situation could

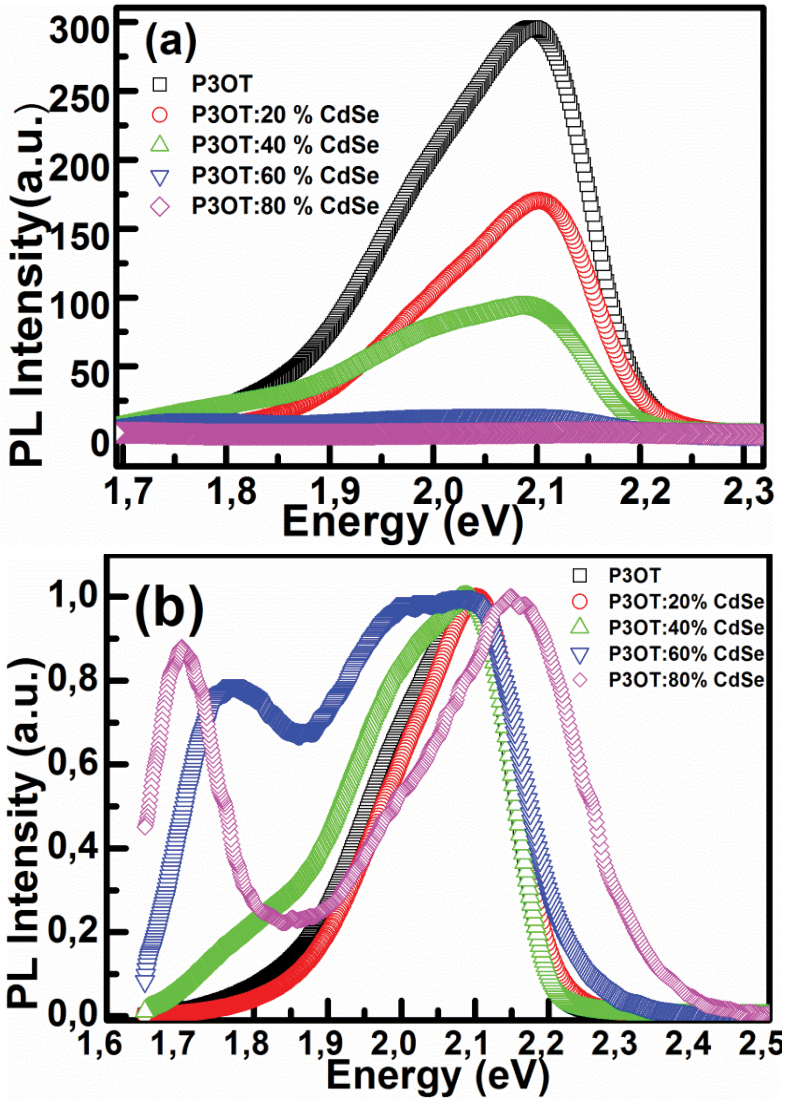

Figure 6: (a) Photoluminescence spectra of P3OT:%CdSe colloidal solutions showing quenching effects. (b) Normalized photoluminescence spectra of P3OT:%CdSe colloidal solutions.

induce a non-radiative energy transfer responsible for emission quenching [55].

It is well established that exciton energy transfer process of this P3OT:%CdSe composite is followed by Förster energy transfer (FRET). FRET arises from the oscillating dipole–dipole interaction that occurs when the donor emission (P3OT emission spectra) overlaps the acceptor absorption (CdSe absorption spectra) as well as to the small distance between the donor and the acceptor, which would be of few nanometers. Noting that both FRET and Förster energy transfers are important in understanding the optoelectronic properties of hybrid nanosystems [56-58]. The key condition for efficient energy transfer is that the absorbance spectrum of acceptor must overlap adequately with the emission spectrum of donor. Figure 7 illustrates this overlap. Figure 8 summarizes the different routes expected for exciton and charge transfer in P3OT:CdSe blend.

In addition, the introduction of CdSe NPs, acting as a modifying agent, may affect the effective conjugation length of P3OT that influences both the dynamics of excited species and recombination. To explain the fluorescence quenching, Ananthakumar, et al. reported that the presence of CdSe in P3HT matrix suppressed the recombination by splitting the charges at the interface, resulting in the production of holes in polymer and electron in CdSe NPs [41].

To shed more light into the role of CdSe NPs and for better comparison, we normalized the PL intensities in Figure 6b. As shown in this figure, no

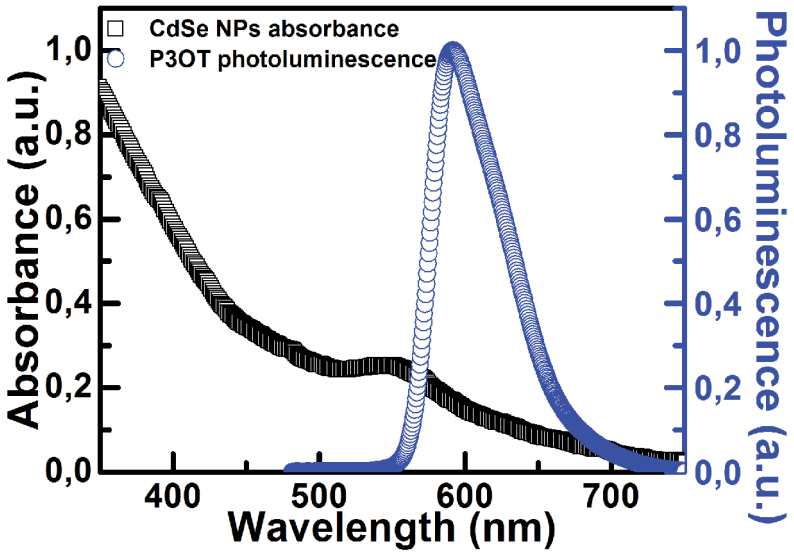

Figure 7: Overlap of CdSe NPs absorbance and P3OT photoluminescence.

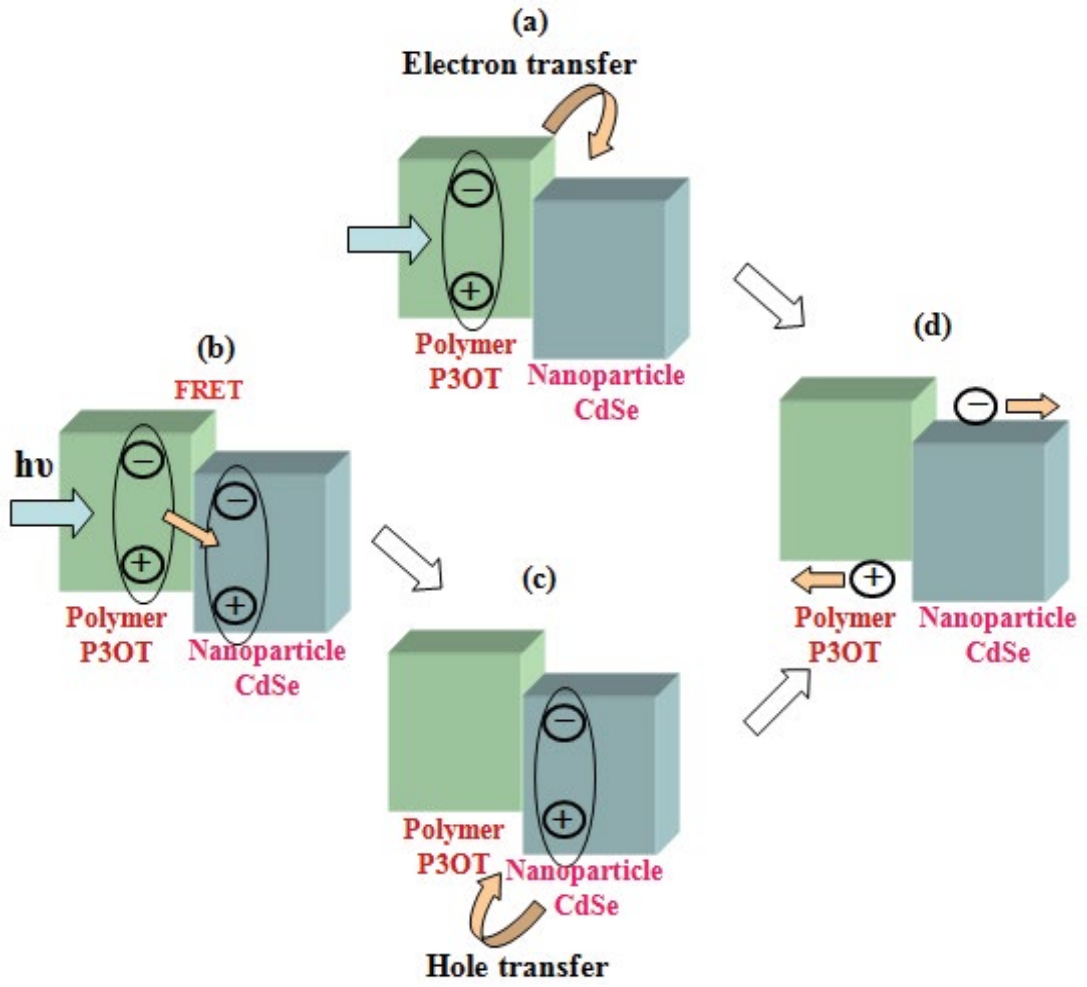

Figure 8: Schematic routes expected for exciton dissociation and charge transfer in P3OT:CdSe composite: (a) Exciton formation in P3OT, followed by electron transfer to CdSe, (b) Exciton formation in P3OT, followed by energy transfer to CdSe, then by hole transfer to P3OT, (c) Exciton formation in CdSe, followed by hole transfer to P3OT (d) Charge separated state.

Citation: Benchaabane A, Lahmar A (2024) Optical Study of Hybrid Colloidal Solution Based on P3OT Polymer and Cdse Nanoparticles. Int J Opt Photonic Eng 9:057

clear change could be observed for P3OT:20%CdSe NPs compared to the pristine P3OT. As soon as the concentration of NPs increases, a clear second band appeared at ca. 2 eV as a shoulder for 40wt% and became clearly visible in P3OT:60%CdSe sample. This feature may be attributed to the emission of a second type of chromophores with shorter conjugation length. However, the second resolved broad band observed for 60 wt% NPs concentration at ca.1.76 eV is a consequence of inter chain interaction. At high CdSe NPs concentration levels, two clear distinct bands are observed at 2.15 and 1.70 eV, respectively. A closer look at these energy values, we suggest that the first emission peak can be attributed to CdSe NPs (see Figure 3). In contrast, the second one, observed at lower energy, may correspond to a small amount of chains-chain aggregation of the P3OT matrix. Note that the existence of two emission centres (yellow/red) could be rationalized in terms of chain packing effects, resulting from the presence of high CdSe-NPs concentration that would create high and low energy chromophores, in agreement with the literature results [42]. A number of processes can result in a decrease of photoluminescence intensity, which is referred to as quenching. In the simplest case, the collisional quenching follows the Stern-Volmer equation [58]:

$$I_0/I = 1 + K_{sv}[Q] \quad (1)$$

Where I_0 and I are the fluorescence intensities observed in the absence and presence of quenchers, respectively, [Q] is the quencher concentration and K_{sv} is the Stern-Volmer quenching constant. The K_{sv} is associated to the excited state lifetime in the absence of quencher τ_0 and the bimolecular quenching rate constant K_q as follows [59]:

$$K_{sv} = K_q \tau_0 \quad (2)$$

Kumari, et al. found straight line plots of I_0/I versus the CdSe concentration [Q] of P3HT and MEH-PPV polymers, respectively by CdSe capped with oleic acid (OA) and CdSe capped with tri-n-octylphosphene-oxide (TOPO) and confirm the occurrence of dynamic quenching [50]. In our case, it is observed that I_0/I plot shows that experimental data result in positive deviation from a linear S-V relation [60-62]. This positive deviation is attributed to various processes such as formation of charge transfer complexes, intersystem crossing, static and dynamic quenching [63].

Recall that for the quenching phenomena in no composite solutions, the fractional intensity (I_0/I) is given by the product of both static and dynamic quenching [64]:

$$I_0/I = (1 + K_{sv}[Q]).(1 + K_s[Q]) \quad (3)$$

Where K_{sv} and K_s the dynamic and static quenching constants, respectively. Figure 9 shows

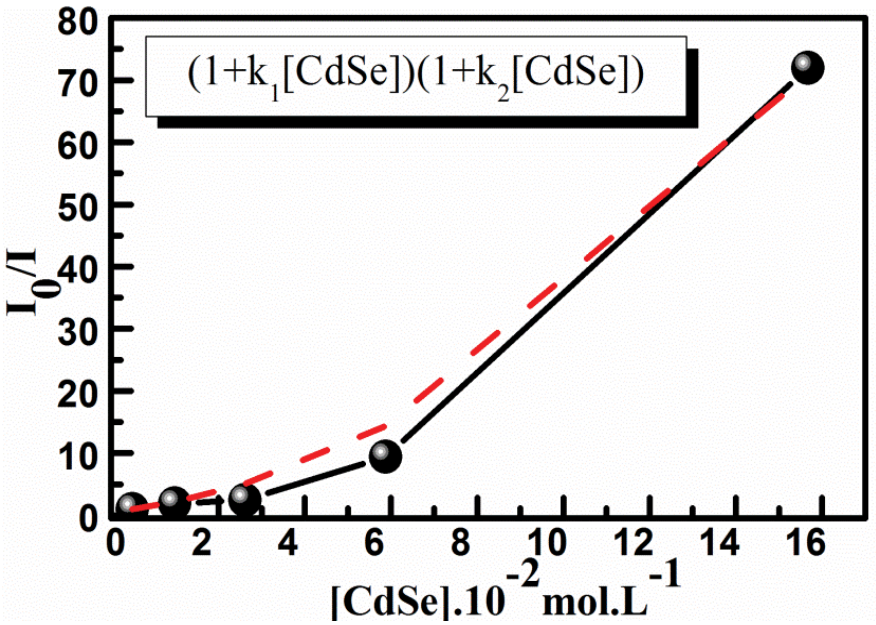

Figure 9: Simultaneous presence of static and dynamic component in the fluorescence quenching. The dash line represents the plot of Eq.(3).

the fraction I_0/I as function of the oleic acid-capped CdSe nanoparticle concentrations for the nanocomposite solutions. A positive deviation was observed in the Stern-Volmer (S-V) plot for both the quenchers. This indicates the presence of either static or transient quenching component in the overall dynamic quenching.

The phenomena being related to the quenching of the host P3OT matrix for which fluorescence decreases even upon the embedding of fraction of oleic acid capped CdSe nanoparticles, is described by Stern-Volmer (S-V) model as evidenced by the fitting of the experimental data according to Eq. (3). The non-radiative complex formation was corroborated by the FTIR data published in a previous work [65]. By applying the above equation, static and dynamic quenching constants are being calculated. The K_{sv} and K_s values are found at 4980 and 7590 $mol.L^{-1}$, respectively. The value found for K_{sv} is in the same order of that reported by Kumar, et al. [66]. It is worthy to mention that dynamic quenching of P3OT polymer nanoparticles by quencher CdSe nanoparticles occurred due to long range electronic energy transfer process, which mainly depends upon the overlap between the absorption spectra of CdSe nanoparticles and the emission spectra of P3OT polymer [67].

Conclusion

Cadmium selenide nanoparticles with diameter of about 8 nm were synthesized and incorporated into poly(3-octylthiophene) conducting polymer. Photoluminescence spectra of P3OT:%CdSe nanocomposite solution based on the embedding of CdSe NPs in P3OT matrix were shown to be mainly governed by P3OT and strongly affected by NPs concentration. It turns out that firstly the NPs act as an efficient quencher for the polymer fluorescence and secondly for high concentration the overall fluorescence spectrum is split out into two separate bands for higher concentrations. The higher energy band corresponds to the NPs photoluminescence and the lower energy one is attributed to the P3OT aggregate emission. This was further confirmed by the Stern-Volmer model which showed the most sound description of P3OT photoluminescence quenching phenomena in P3OT:%CdSe nanocomposite solution. The energy transfer accompanying this quenching process, which is of FRET type, results in an efficient fluorescence of CdSe NPs. However, the photoluminescence quenching mechanism would be restricted by the presence of residual ligand species and phase segregation effects in P3OT:CdSe nanocomposite.

Conflicts of Interest

There are no conflicts to declare.

References

1. Wang M, Kee S, Barker D, Travas-Sejdic J (2020) Highly stretchable, solution-processable, and crosslinkable poly(3,4-ethylenedioxithiophene)-based conjugated polymers. Euro Polym J 125: 109508.
2. Zheng N, Lin Z, Zheng Y, Li D, Yang J, et al. (2020) Room-temperature stable organic spin valves using solution-processed ambipolar naphthalene diimide-based conjugated polymers. Org Electron 81: 105684.
3. Wong Y-T, Lin P-C, Tseng C-W, Huang Y-W, Su Y-A, et al. (2020) Biaxially-extended side-chain engineering of benzodithiophene-based conjugated polymers and their applications in polymer solar cells. Org Electron 79: 105630.
4. Ashizawa M, Zheng Y, Tran H, Bao Z (2020) Intrinsically stretchable conjugated polymer semiconductors in field effect transistors. Prog in Polym Sci 100: 101181.
5. Handa NV, Serrano AV, Robb MJ, Hawker CJ (2015) Exploring the synthesis and impact of end-functional poly(3-hexylthiophene). J Polym Sci Part A: Polym Chem 53: 831-841.
6. Bousquet A, Awada H, Hiorns RC, Dagron-Lartigau C, Billon L (2014) Conjugated-polymer grafting on inorganic and organic substrates: A new trend in organic electronic materials. Prog Polym Sci 39: 1847-1877.
7. Thomas A, Tom AE, Ison VV (2022) An inverted architecture P3HT:CdSe bulk-heterojunction hybrid solar cell utilizing a quantum junction with high open circuit voltage and efficiency. Energy Reports 8: 12979-12986.
8. Shrestha NK, Yoon SJ, Bathula C, Opoku H, Noh Y-Y (2019) Hole-induced polymerized interfacial film of polythiophene as co-sensitizer and back-electron injection barrier layer in dye-sensitized TiO_2 nanotube array. J Alloys Compd 781: 589-594.
9. Morales-Espinoza EG, Ruiu A, Valderrama-García BX, Duhamel J, Rivera E (2019) Design, characterization, optical and photophysical properties of novel thiophene monomers and polymers containing pyrene moieties linked via rigid and flexible spacers. Synth Met 248: 102-109.

10. Al Zoubi W, Kamil MP, Fatimah S, Nashrah N, Ko YG (2020) Recent advances in hybrid organic-inorganic materials with spatial architecture for state-of-the-art applications. Prog Mater Sci 112: 100663.

11. Zhang C, Yu P-L, Jian-Chang YL (2020) Polymer/TiO_2 nanoparticles interfacial effects on resistive switching under mechanical strain. Org Electron 77: 105528.

12. Zhu X, Guo B, Jin F, Zhai T, Wang Y, et al. (2019) Surface modification of ZnO electron transport layers with glycine for efficient inverted non-fullerene polymer solar cells. Org Electron 70: 25-31.

13. Jaimes W, Alvarado-Tenorio G, Martínez-Alonso C, Quevedo-López A, Hailin Hu, et al. (2015) Effect of CdS nanoparticle content on the in-situ polymerization of 3-hexylthiophene-2,5-diylandthe application of P3HT-CdS products in hybrid solar cells. Mater Sci Semicond Process 37: 259-265.

14. Bhattacharyya S, Patra A (2014) Interactions of Π-conjugated polymers with inorganic nanocrystals. J of Photochem and Photobio C: Photochem Rev 20: 51-70.

15. Salim E, Bobbara SR, Oraby A, Nunzi JM (2019) Copper oxide nanoparticle doped bulk-heterojunction photovoltaic devices. Synth Met 252: 21-28.

16. Benchaabane A, Ben Hamed Z, Kouki F, Sanhoury MA, Zellama K, et al. (2014) Performances of effective medium model in interpreting optical properties of polyvinylcarbazole:ZnSe nanocomposite. J Appl Phys 115: 134313.

17. Yoon C, Yang KP, Kim JW, Shin K, Lee K (2020) Fabrication of highly transparent and luminescent quantum dot/polymer nanocomposite for light emitting diode using amphiphilic polymer-modified quantum dots. Chem Eng J 382: 122792.

18. Benchaabane A, Ben Hamed Z, Sanhoury MA, Kouki F, Zeinert A, et al. (2016) Influence of nanocrystal concentration on the performance of hybrid P3HT:TBPO-capped CdSe nanocrystal solar cells. Appl Phys A 122: 60.

19. Kim S, Park H, Kang MS (2022) Semi-interpenetrating network of polymer semiconductor and tetrapod nanocrystal assemblies with balanced ambipolar transport. Materials Chemistry and Physics 287: 126300.

20. Ayesh AI, Salah B, Al-Sulaiti LA (2020) Production and characterization of flexible semiconducting polymer nanoparticle composites for x-ray sensors. Rad Phys Chem 167: 108233.

21. Benchaabane A, Ben Hamed Z, Telfah A, Sanhoury MA, Kouki F, et al. (2017) Effect of OA-ZnSe nanoparticles incorporation on the performance of PVK organic photovoltaic cells. Mater Sci Semicond Process 64: 115-123.

22. Kesavan AV, Kumar MP, Rao AD, Ramamurthy PC (2019) Light management through up-conversion and scattering mechanism of rare earth nanoparticle in polymer photovoltaics. Opt Mater 94: 286-293.

23. Benchaabane A, Hajlaoui ME, Hnainia N, Al-Tabbakh A, Zeinert A, et al. (2020) Optical properties enhancement of hybrid nanocomposites thin films based on P3HT matrix and ZnO@SiO_2 core-shell nanoparticles. Opt Mater 102: 109829.

24. Elain Hajlaoui M, Hnainia N, Gouid Z, Benchaabane A, Sanhoury MA, et al. (2020) Optimization of hybrid P3HT:CdSe photovoltaic devices through surface ligand modification. Mater Sci Semicond Process 109: 104934.

25. Hebestreit N, Hofmann J, Rammelt U, Plieth W (2003) Electrochemical characterization of nanocomposites formed from polythiophene, titanium dioxide. Electrochim Acta 48: 1779-1788.

26. Sharma GD, Suresh P, Sharma SK, Roy MS (2008) Optical electrical properties of hybrid photovoltaic devices from poly(3-phenyl hydrazonethiophene) (PPHT) TiO_2 blend films. Sol Ener Mater Sol Cells 92: 61-70.

27. Huisman CL, Goossens A, Schoonman J (2003) Preparation of an nanostructured composite of titanium dioxide and polythiophene: A new route towards 3D heterojunction solar cells. Synth Met 138: 237-241.

28. Spanggaard H, Krebs FC (2004) A brief history of the development of organic and polymeric photovoltaics. Sol Ener Mater Sol Cells 83: 125-146.

29. Boufflet P, Casey A, Xia Y, Stavrinou PN, Heeney M (2017) Pentafluorobenzene end-group as a versatile handle for para fluoro “click” functionalization of polythiophenes. Chem Sci 8: 2215-2225.

30. Bullen CR, Mulvaney (2004) Nucleation and growth kinetics of CdSe nanocrystals in Octadecene. Nano Lett 12: 2303-2307.

31. Yang YA, Wu H, Williams KR, Cao YC (2005) Synthesis of CdSe and CdTe Nanocrystals without precursor injection. Angew Chem Int Ed Engl 44: 6712-6715.

32. Benchaabane, Ben Hamed Z, Kouki F, Zeinert A, Bouchriha H (2015) Photogeneration process in bulk heterojunction solar cell based on quaterthiophene and CdS nanoparticles. Appl Phys A 120: 1149-1157.

33. Moule AJ, Meerholz K (2009) Morphology control in solution-processed Bulk-Heterojunction solar cell mixtures. Adv Funct Mater 19: 3028-3036.

34. Kanemoto K, Sudo T, Akai I, Hashimoto H, Karasawa T, et al. (2006) Intrachain photoluminescence properties of conjugated polymers as revealed by long oligothiophenes and polythiophenes diluted in an inactive solid matrix. Phys Rev B 73: 235203.

35. Reiss P, Couderc E, Girolamo JD, Porn A (2011) Conjugated polymers/semiconductor nanocrystals hybrid materials preparation, electrical transport properties and applications. Nanoscale 3: 446-489.

36. Chen G, Seo J, Yang C, Prasad PN (2013) Nanochemistry and nanomaterials for photovoltaics. Chem Soc Rev 42: 8304-8338.

37. Hajlaoui ME, Dhahri R, Hnainia N, Benchaabane A, Dhahri E, et al. (2020) Dielectric spectroscopy study of the Ni0.2Zn0.8Fe2O4 spinel ferrite as a function of frequency and temperature. Mater Sci Eng B 262: 114683.

38. Zhao Y, Yan Z, Liu J, Wei A (2013) Synthesis and characterization of CdSe nanocrystalline thin films deposited by chemical bath deposition. Mater Sci Semicond Process 16: 1592-1598.

39. Zhu J, Liao X, Zhao X, Wang J (2001) Photochemical synthesis and characterization of CdSe nanoparticles. Mater Lett 47: 339-343.

40. Okamoto K, Vyawahare S, Scherer A (2006) Surface-plasmon enhanced bright emission from CdSe quantum-dot nanocrystals. J Opt Soc Am B 23: 1674-1678.

41. Ananthakumar S, Ramkumar J, Moorthy Babu S (2014) Synthesis of thiol modified CdSe nanoparticles/P3HT blends for hybrid solar cell structures. Mater Sci Semicond Process 22: 44-49.

42. Palacios RE, Barbara PF (2007) Single molecule spectroscopy of poly 3-octyl thiophene (P3OT). J Fluoresc 17: 749-757.

43. Tirapattur S, Belletête M, Drolet N, Leclerc M, Durocher G (2003) Steady-state and time-resolved studies of 2,7-carbazole-based conjugated polymers in solution and as thin films: Determination of their solid state fluorescence quantum efficiencies. Chem Phys Lett 370: 799-804.

44. Pizani PS, Leite ER, Pontes FM, Paris EC, Rangel JH, et al. (2000) Photoluminescence of disordered ABO_3 perovskites. Appl Phys Lett 77: 824.

45. Kouki F, Spearman P, Valat P, Horowitz G, Garnier F (2000) Experimental determination of excitonic levels in a-oligothiophenes. J Chem Phys 113: 385-391.

46. Silva TH, Barreira SVP, Moura C, Silva F (2003) Characterization of a self-assembled polyelectrolyte film. Electrochim Acta 21: 281.

47. Skompska M, Szkurlat A (2001) The influence of the structural defects and microscopic aggregation of poly(3-alkylthiophenes) on electrochemical and optical properties of the polymer films: discussion of an origin of redox peaks in the cyclic voltammograms. Electrochim Acta 46: 4007-4015.

48. Nascimento CA, Schura AB, Chagas EF, Ramos RJ, de Santana H, et al. (2020) Inter- and intrachain transition analyses by photoluminescence and Raman Spectroscopy of electrochemically synthesized P3OT films. Journal of Mater Sci Mater in Electron 31: 6629-6635.

49. Hamed ZB, Benchaabane A, Kouki F, Sanhoury MA, Bouchriha H (2014) Fluorescence quenching in PVK:ZnSe nanocomposite structure. Synth Met 195: 102-109.

50. Kumari K, Kumar U, Sharma SN, Chand S, Kakkar R, et al. (2008) Effect of surface passivating ligand on structural and optoelectronic properties of polymer:CdSe quantum dot composites. J Phys D: Appl Phys 41: 235409.

51. Sharma SN, Sharma RK, Lakshmikumar ST (2005) Role of an electrolyte and substrate on the stability of porous silicon. Physica E: Low-dimensional Systems and Nanostructures 28: 264-272.

52. Geru II, Bordian OT, Culeac IP, Verlan VI (2015) CdSe quantum dots and SBMA/CdSe nanocomposites characterization by optical and 2D DOSY NMR methods. Univ J Phys Appl 9: 263-272.

53. Motta FV, Marques APA, Espinosa JWM, Pizani PS, Longo E, et al. (2010) Room temperature photoluminescence of BCT prepared by Complex Polymerization Method. Curr Appl Phys 10: 16-20.

54. Xiong H-M (2010) Photoluminescent ZnO nanoparticles modified by polymers. J Mater Chem 20: 4251-4262.

55. Sharma SN, Vats T, Dhenadhayalan N, Ramamurthy P, Narula AK (2012) Ligand-dependent transient absorption studies of hybrid polymer: CdSe quantum dot composites. Sol Ener Mater Sol Cells 100: 6-15.

56. Lee Y-B, Lee SH, Park S-Y, Park C-J, Lee K-S, et al. (2014) Luminescence enhancement by surface plasmon assisted Förster resonance energy transfer in quantum dots and light emitting polymer hybrids with Au nanoparticles. Synth Met 187: 130-135.

57. Förster T (1959) 10th Spiers Memorial Lecture. Transfer mechanisms of electronic excitation, Discuss Faraday Soc, 27: 7-17.

58. Al-Asbahi BA, Jumali MHH, Yap CC, Flaifel MH, Salleh MM (2013) Photophysical properties and energy transfer mechanism of PFO/Fluorol 7GA hybrid thin films. J Lumin 142: 57-65.

59. Bertoncello P, Notargiacomo A, Nicolini C (2004) Synthesis, fabrication and characterization of poly[3-3_(vinylcarbazole)] (PVK) Langmuir-Schaefer films. Polym 45: 1659-1664.

60. Hanagodimath SM, Gadaginmath GS, Chikkur GC (1990) Environmental effects on the energy migration coefficient, the effective energy transfer and quenching distances in an organic liquid scintillator. Chem Phys 148: 347-357.

61. Giraddi TP, Kadadevaramath JS, Malimath GH, Chikkur GC (1996) Effect of solvent on the fluorescence quenching of organic liquid scintillators by aniline and carbon tetrachloride. Appl Radiat Isot 47: 461-466.

62. Shailaja MK, Hanagodimath SM, Kadadevaramath JS, Chikkur GC (2000) Photocyclization Reactions of (ω-Phthalimidoalkoxy) acetic acids via sequential single electron transfer-Decarboxylation pathways. J Photoscience 6: 159.

63. Thipperudrappa J, Biradar DS, Hanagodimath SM (2007) Simultaneous presence of static and dynamic component in the fluorescence quenching of Bis-MSB by CCl4 and aniline. J Lumin 124: 45-50.

64. Lakowicz JR (1986) Principle of lluorescence spectroscopy. Plenum Press, New York, London, 266.

65. Benchaabane A, Belhadi J, Ben Hamed Z, Lejeune M, Lahmar A, et al. (2016) Effect of CdSe nanoparticles incorporation on the performance of P3OT organic photovoltaic cells. Mater Sci Semicond Process 41: 343-349.

66. Kumar S, Kumar J, Narayan Sharma S, Srivastava S (2018) rGOintegrated MEHPPV and P3HT polymer blends for bulk hetero junction solar cells: A comparative insight. Optik 178: 411-421.

67. Bhattcharyya S, Patra A (2012) Photoluminescence quenching of semiconducting polymer nanoparticles in presence of Au nanoparticles. Bull Mater Sci 35: 719-725.

DOI: 10.35840/2631-5092/4557